Trans. SHASE
No. 30, Feb., 1985

Evaluation of Ventilation Systems through Three Dimensional Numerical Computation

By Yoshiaki Ishizu*

Synopsis: To make an evaluation of ventilation systems, numerical computation was carried out for three dimensional, isothermal, and turbulent flow schemes. It was found that there exists an optimum position for an inlet in relation to an outlet whereby the most effective ventilation can be attained. In addition, similar to the results for the two dimensional computation, the slope of the concentration decay is virtually constant and independent of the position in the room, so the mixing factor derived from this slope can be used as an index of the ventilation efficiency. Further, three dimensional computation seems to be necessary for a quantitative estimation of the mixing factor.

Introduction

In addition to temperature and humidity, there has been an increased concern for the cleanliness of indoor air. The cleanliness of indoor air can readily be improved by increasing the ventilation rate. However, this method is not desirable from the viewpoint of energy conservation. Instead, more light should be thrown on the effectiveness of ventilation systems. In a previous paper[1], the effects of the inlet and the outlet positions on the ventilation efficiency were examined through two dimensional computation.

In this paper, numerical computation has been extended to three dimensions and the results are discussed from the viewpoint of the ventilation efficiency. Furthermore, the index for ventilation efficiency which was proposed for the two dimensional model has been found to be suitable in three dimensional model as well.

* Central Research Institute, Japan Tobacco Inc., Member

1. Nomenclature

C : Concentration
C_0 : Initial concentration of pollutant in room
D : Effective turbulent diffusion coefficient
G : Pollutant generation rate
k : Kinetic energy of turbulence
l_0 : Width of inlet
m : Mixing factor
P : Pressure
p : Position factor
Q : Air flow rate
t : Time
u, v, w : Component of mean velocity in directions x, y and z
w_0 : Flow velocity at inlet
V : Volume of room
x, y, z : Cartesian space coordinate

Greek Symbols

Γ_k : Effective turbulent diffusion coefficient for diffusion of $k(=\nu_0+\Gamma_{k,t})$
$\Gamma_{k,t}$: Turbulent diffusion coefficient for diffu-

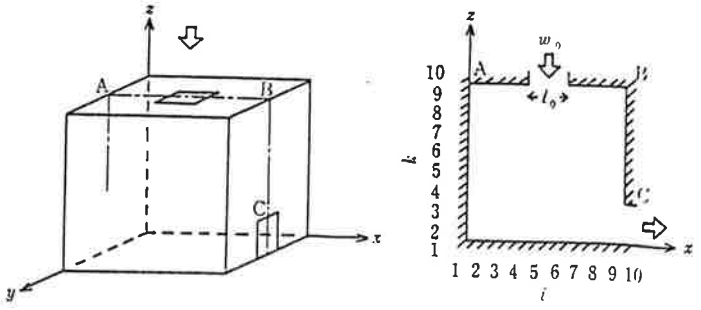

Fig. 1 Basic room model and the coordinate system

sion of $k(=\nu_t/\sigma_k)$

Γ_ε : Effective turbulent diffusion coefficient for diffusion of $\varepsilon(=\nu_0+\Gamma_{\varepsilon,t})$

$\Gamma_{\varepsilon,t}$: Turbulent diffusion coefficient for diffusion of $\varepsilon(=\nu_t/\sigma_\varepsilon)$

ε : Turbulence energy dissipation rate

ν : Effective turbulent kinematic viscosity $(=\nu_0+\nu_t)$

ν_0 : Kinematic viscosity

ν_t : Turbulent kinematic viscosity

$\sigma_1, \sigma_2, \sigma_\mu$: Coefficients in approximated turbulent transport equations

$\sigma_k, \sigma_\varepsilon, \sigma_C$: Turbulent Schmidt number corresponding to k, ε, C

ϕ : Generalized dependent variable

2. Calculation method

Numerical Calculation was carried out for three dimensional, isothermal, and turbulent flow schemes with the coordinate system sown in **Fig. 1**. The basic equations are as follows[2),3)].

1) Continuity equation

$$\frac{\partial u}{\partial x}+\frac{\partial v}{\partial y}+\frac{\partial w}{\partial z}=0 \qquad \cdots\cdots(1)$$

2) Momentum equation

$$\frac{\partial(uu)}{\partial x}+\frac{\partial(uv)}{\partial y}+\frac{\partial(uw)}{\partial z}=-\frac{\partial P}{\partial x}+\frac{\partial}{\partial x}\left(\nu\frac{\partial u}{\partial x}\right)+\frac{\partial}{\partial y}\left(\nu\frac{\partial u}{\partial y}\right)+\frac{\partial}{\partial z}\left(\nu\frac{\partial u}{\partial z}\right)+S_u \qquad \cdots\cdots(2)$$

$$\frac{\partial(uv)}{\partial x}+\frac{\partial(vv)}{\partial y}+\frac{\partial(vw)}{\partial z}=-\frac{\partial P}{\partial y}+\frac{\partial}{\partial x}\left(\nu\frac{\partial v}{\partial x}\right)+\frac{\partial}{\partial y}\left(\nu\frac{\partial v}{\partial y}\right)+\frac{\partial}{\partial z}\left(\nu\frac{\partial v}{\partial z}\right)+S_v \qquad \cdots\cdots(3)$$

$$\frac{\partial(uw)}{\partial x}+\frac{\partial(vw)}{\partial y}+\frac{\partial(ww)}{\partial z}=-\frac{\partial P}{\partial z}+\frac{\partial}{\partial x}\left(\nu\frac{\partial w}{\partial x}\right)+\frac{\partial}{\partial y}\left(\nu\frac{\partial w}{\partial y}\right)+\frac{\partial}{\partial z}\left(\nu\frac{\partial w}{\partial z}\right)+S_w \qquad \cdots\cdots(4)$$

where,

$$S_u=\frac{\partial}{\partial x}\left(\nu\frac{\partial u}{\partial x}\right)+\frac{\partial}{\partial y}\left(\nu\frac{\partial v}{\partial x}\right)+\frac{\partial}{\partial z}\left(\nu\frac{\partial w}{\partial x}\right) \qquad \cdots\cdots(5)$$

$$S_v=\frac{\partial}{\partial x}\left(\nu\frac{\partial u}{\partial y}\right)+\frac{\partial}{\partial y}\left(\nu\frac{\partial v}{\partial y}\right)+\frac{\partial}{\partial z}\left(\nu\frac{\partial w}{\partial y}\right) \qquad \cdots\cdots(6)$$

$$S_w=\frac{\partial}{\partial x}\left(\nu\frac{\partial u}{\partial z}\right)+\frac{\partial}{\partial y}\left(\nu\frac{\partial v}{\partial z}\right)+\frac{\partial}{\partial z}\left(\nu\frac{\partial w}{\partial z}\right) \qquad \cdots\cdots(7)$$

3) k-equation

$$\frac{\partial(uk)}{\partial x}+\frac{\partial(vk)}{\partial y}+\frac{\partial(wk)}{\partial z}=\frac{\partial}{\partial x}\left(\Gamma_k\frac{\partial k}{\partial x}\right)+\frac{\partial}{\partial y}\left(\Gamma_k\frac{\partial k}{\partial y}\right)+\frac{\partial}{\partial z}\left(\Gamma_k\frac{\partial k}{\partial z}\right)+\nu_t S-\sigma_\mu k^2/\nu_t \qquad \cdots\cdots(8)$$

4) ε-equation

$$\frac{\partial(u\varepsilon)}{\partial x}+\frac{\partial(v\varepsilon)}{\partial y}+\frac{\partial(w\varepsilon)}{\partial z}=\frac{\partial}{\partial x}\left(\Gamma_\varepsilon\frac{\partial\varepsilon}{\partial x}\right)+\frac{\partial}{\partial y}\left(\Gamma_\varepsilon\frac{\partial\varepsilon}{\partial y}\right)+\frac{\partial}{\partial z}\left(\Gamma_\varepsilon\frac{\partial\varepsilon}{\partial z}\right)+\sigma_1\sigma_\mu kS-\sigma_1\varepsilon^2/k \qquad \cdots\cdots(9)$$

where,

$$S=2\left\{\left(\frac{\partial u}{\partial x}\right)^2+\left(\frac{\partial v}{\partial y}\right)^2+\left(\frac{\partial w}{\partial z}\right)^2\right\}+\left(\frac{\partial u}{\partial y}+\frac{\partial v}{\partial x}\right)^2+\left(\frac{\partial v}{\partial z}+\frac{\partial w}{\partial y}\right)^2+\left(\frac{\partial w}{\partial x}+\frac{\partial u}{\partial z}\right)^2 \qquad \cdots\cdots(10)$$

5) Concentration equation

$$\frac{\partial(uC)}{\partial x}+\frac{\partial(vC)}{\partial y}+\frac{\partial(wC)}{\partial z}=\frac{\partial}{\partial x}\left(D\frac{\partial C}{\partial x}\right)+\frac{\partial}{\partial y}\left(D\frac{\partial C}{\partial y}\right)+\frac{\partial}{\partial z}\left(D\frac{\partial C}{\partial z}\right)+G \qquad \cdots\cdots(11)$$

where,

$$\left.\begin{aligned}&\nu=1/Re+\nu_t, && \nu_t=\sigma_\mu k^2/\varepsilon\\ &\Gamma_k=1/Re+\nu_t/\sigma_k, && \Gamma_\varepsilon=1/Re+\nu_t/\sigma_\varepsilon\\ &D=1/(ReSc)+\nu_t/\sigma_C\end{aligned}\right\} \qquad \cdots\cdots(12)$$

All of the parameters have been made nondimensional with the characteristic length being the width of the inlet, l_0, the characteristic velocity being the flow rate at the inlet, w_0, and the characteristic concentration being that of exhaust air. The constants used were the values recommended by Launder et al. which are shown in **Table 1**. The Reynolds number, Re, and Schmidt number, Sc, were assigned the values 1.0×10^4 and

0.9, respectively.

The basic equations were solved by the finite approximation method after Yamaguchi[3]. Considering the computation time, calculation mesh grid was set $10\times10\times10$ including the imaginary control volume beyond the walls. Calculations for the steady state were terminated when the maximum value of the relative change of each parameter at every point in the room

$$\left|\frac{\phi^N-\phi^{N-1}}{\phi^N}\right|^{i,j}_{\max} ; \phi=u, v, w, P, k, \varepsilon, C$$

became smaller than 1.0×10^{-4}.

After obtaining the steady state solution, pollutant generation was stopped and the decay of the concentration with time was calculated by the A. D. I. method. The flow itself was kept in the steady state. In this case, $\partial C/\partial t$ was added to the left hand side of the concentration equation (11). Since the change in concentration with time is rapid at first and slow afterwards, the time increment Δt was made to increase in geometric ratio with the initial interval, 0.1, and the common ratio, 1.01. The position of the outlet was fixed at the bottom of the right wall and the position of the inlet was successively changed on the ceiling. The shape of the inlet and the outlet is square with a side being 1/4 of that of the room. For these calculations, the pollutant generation site was fixed at the center of the room at (5, 5, 3).

In addition, the concentration distribution was calculated for various pollutant generation sites in a room with fixed inlet and outlet positions. Calculations were performed on a Vax-11/750 super minicomputer made by DEC Co. Ltd.

3. Results

The distributions of flow and concentration at the cross section $j=5$ are shown in **Fig. 2** through 4. When the inlet is at the leftmost position on the ceiling, the main part of the air flows down the left wall and across the floor, purging the pollutant from the room effectively. Thus, the average concentration in the room becomes relatively low. When the inlet is at the rightmost position on the ceiling, the main part of the flow goes down the right wall and flows out of the outlet without mixing with the room air. Consequently, some air with a high concentration stagnates in the room and the average concentration becomes high. Even though the inlet and the outlet positions are fixed, the concentration depends also on the pollutant generation site. As shown in **Fig. 5**, some air with a high concentration stays in the room when the pollutant generation site is far from the outlet. If the pollutant generation site is near the outlet, the pollutant is likely to be purged. Thus the concentration doesn't become so high as shown in **Fig. 6**.

Table 1 Constants used for numerical calculation

σ_μ	σ_1	σ_2	σ_k	σ_ε	σ_C
0.09	1.44	1.92	1.0	1.3	0.9

After the termination of pollutant generation, the concentration of the pollutant decays. Six sites were chosen as representative ones in the room, and the concentration decay at these sites was plotted on semilogarithmic graphs as shown in **Figs. 7** through 9. It seems, from these figures, that the slope of the concentration decay becomes virtually constant after some initial perturbations, allowing for a very slight curvature of the lines.

4. Discussion

While pollutant generation continues, the concentration is extremely high at the pollutant generation site. After the termination of pollutant generation, the singularity of the pollutant generation site disappears and the concentration distribution rapidly approaches the distribution which depends only on the flow pattern in the room, governed mainly by the inlet and the outlet positions. When the flow is in steady state, it is expected that the relative distribution of the concentration becomes not to change with respect to time. Thus the pattern of the concentration decay will become the same throughout the room. The results of the numerical computation confirmed this expectation. As shown in **Figs. 7** to 9, the decay of the concentration can be expressed by virtually the straight line on a semilogarithmic

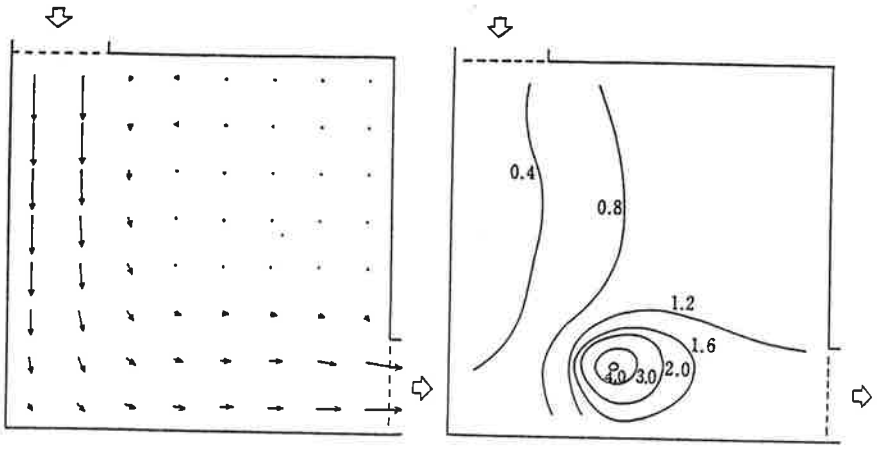

Fig. 2 Crosssectional view of the air flow and the concentration at $j=5$ when the inlet is at the leftmost position on the ceiling

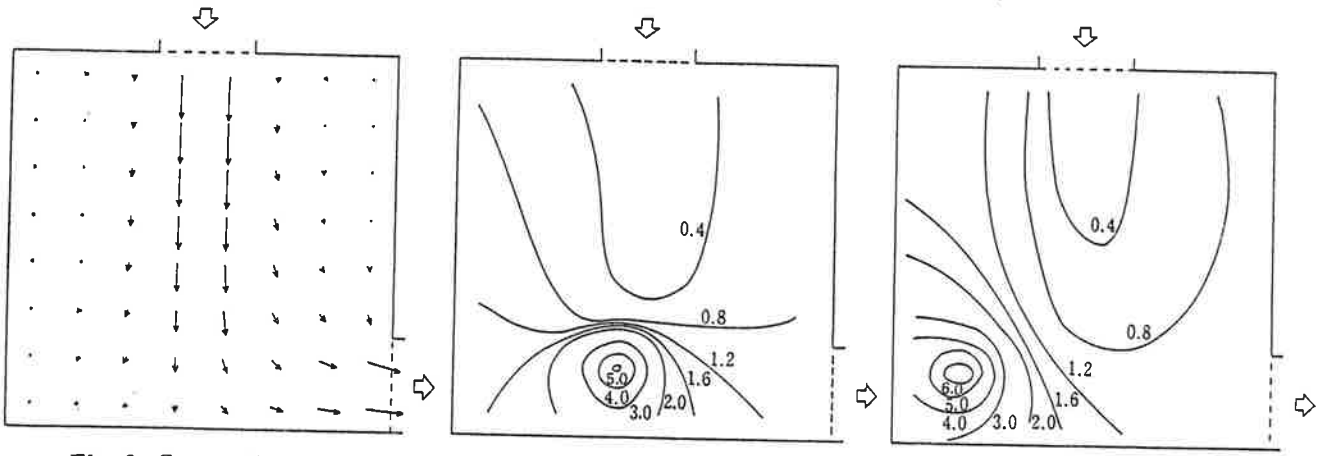

Fig. 3 Crosssectional view of the air flow and the concentration at $j=5$ when the inlet is at the center of the ceiling

Fig. 5 Crosssectional view of the concentration at $j=5$ when the pollutant generation site is far from the outlet. Air flow is the same as that in **Fig. 3.**

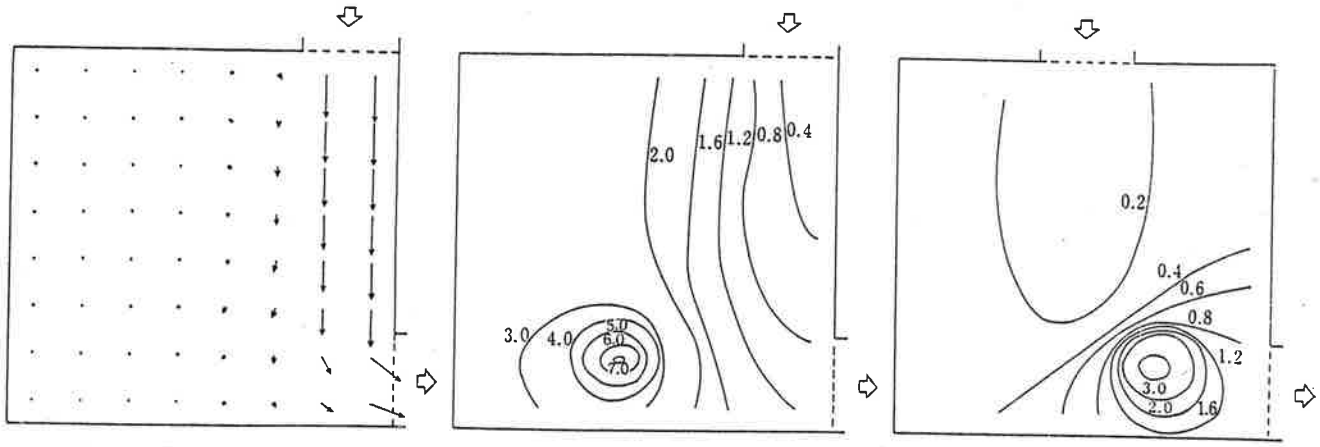

Fig. 4 Crosssectional view of the air flow and the concentration at $j=5$ when the inlet is at the rightmost position on the ceiling

Fig. 6 Crosssectional view of the concentration at $j=5$ when the pollutant generation site is near the outlet. Air flow is the same as that in **Fig. 3.**

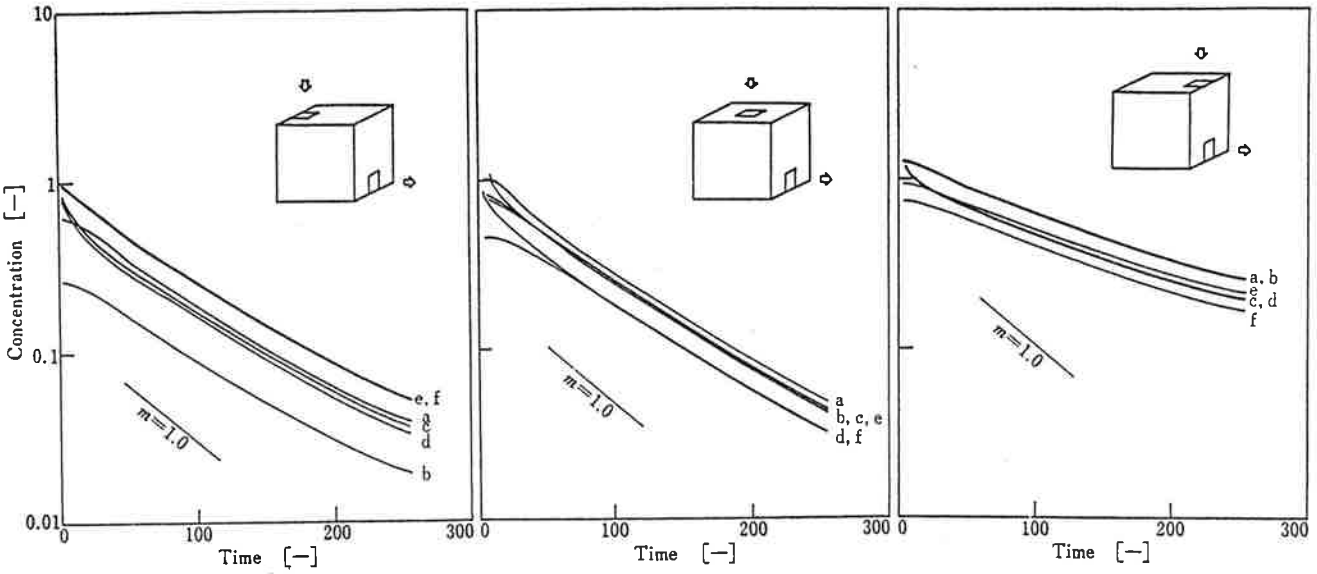

Fig. 7 Concentration decay with time when the inlet is at the leftmost position on the ceiling ; a(3, 3, 7), b(3, 5, 7), c(5, 3, 3), d(5, 5, 3), e(7, 3, 7), f(7, 5, 7)

Fig. 8 The same as **Fig. 7** when the inlet is at the center of the ceiling

Fig. 9 The same as **Fig. 7** when the inlet is at the rightmost position on the ceiling

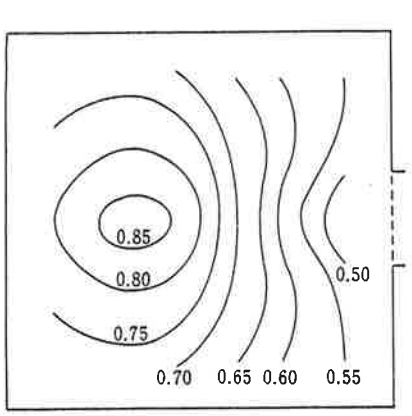

Fig. 10 Dependence of the mixing factor m upon the inlet position. The outlet position is fixed at the bottom of the right wall.

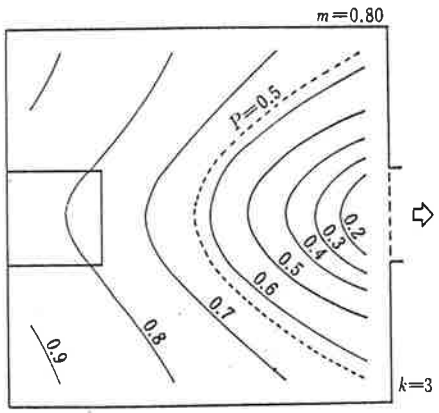

Fig. 11 The average concentration in the steady state, $C_\infty = p/m$, as a function of the pollutant generation site whose height is fixed at $k=3$. The inlet is at the leftmost position on the ceiling. P represents the position factor.

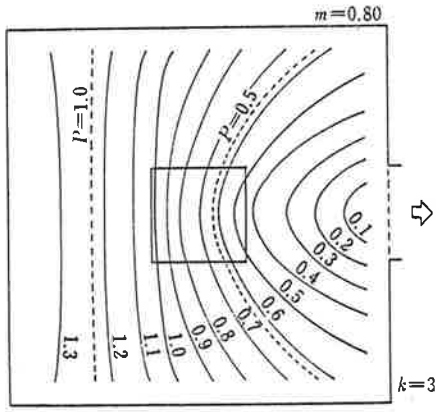

Fig. 12 The same as **Fig. 11** when the inlet is at the center of the ceiling

graph, similar to the results in two dimensional computation[1]. Accordingly, the change in the concentration at each point in a room can be expressed by the equation $C=C_0 \exp(-mQt/V)$. Here, C_0 is the initial concentration, Q is the volumetric flow rate of the supplied air, V is the volume of the room, and t is time. The character m stands for the mixing factor which represents the ventilation efficiency. We assume that the mQ portion of the supplied air, Q, mixes completely with the room air and the rest portion $(1-m)Q$ flows out without mixing. For reference, the slope of the concentration decay with complete mixing, $m=1.0$, is also shown in **Figs. 7** to **9**.

The mixing factors derived from the slope of the concentration decay, by taking the linear regression during the time period of about 50 to 150, are summarized in **Fig. 10**. If the outlet position

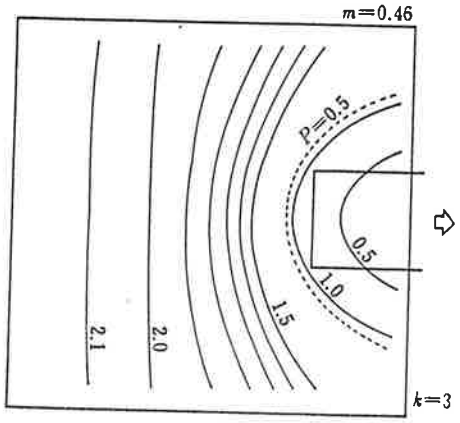

Fig. 13 The same as **Fig. 11** when the inlet is at the rightmost position on the ceiling

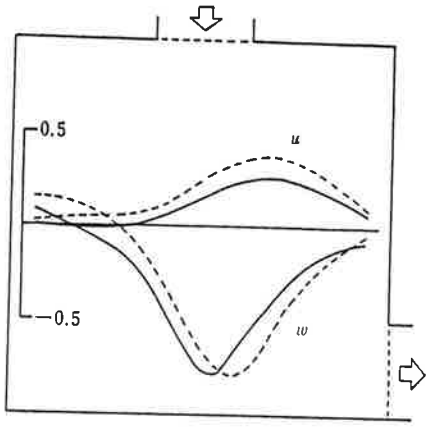

Fig. 14 Comparison of the velocity distributions calculated in two dimensional scheme (broken lines) with three dimensional one (solid lines)

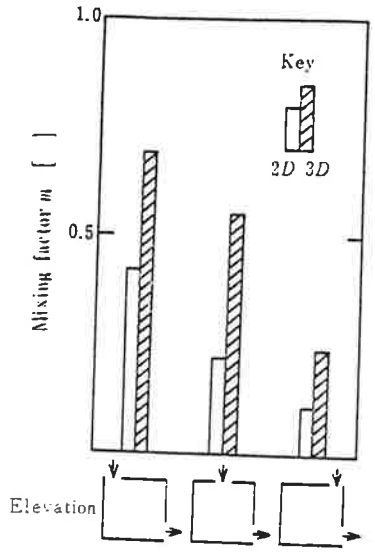

Fig. 15 Comparison of the mixing factor calculated in two dimensional scheme with three dimensional one

is fixed at the bottom of the right wall, the mixing factor becomes highest when the inlet is near the center rather than the farthest left. In other words, fresh air is most effectively used to clean the room air when the inlet is at this site. When the inlet is on the right part of the ceiling, a considerable part of the supplied air goes out without mixing with the room air, and thus the mixing factor becomes smaller.

It was found that the mixing factor was independent of the pollutant generation site in the three dimensional computation just as it was in the two dimensional one. This makes the mixing factor a very promising and reasonable index for expressing the ventilation efficiency, because ventilation is the idea which should not be affected by the pollutant generation site.

The average concentration of pollutant in a room depends also on the pollutant generation site. Thus we defined "position factor" p as an index showing the effect of the pollutant generation site. Position factor was assumed such that pV portion of the room is polluted with complete mixing, while $(1-p)V$ portion of the room is occupied by fresh air. Then the average concentration of the room in steady state can be expressed by $pG/(mQ)$[1]. It should be noticed that even when G and Q are fixed, the average concentration can be reduced by decreasing the factor p and/or increasing the factor m. In **Fig. 11**, contours of the average concentration in steady state with unit pollutant generation rate and unit ventilation rate, that is $C_\infty = p/m$, is shown as a function of the pollutant generation site. The inlet is at the leftmost position on the ceiling. Since the mixing factor m is constant throughout the room when the inlet and the outlet positions are definite, and the position factor p is expressed by mC_∞, a contour similar to that of C_∞ can be drawn for p. As a representative example, a contour of $p=0.5$ is shown in the figure. In other words, when the pollutant generation site is upon this broken line, position factor p becomes 0.5. Similar contours are shown in **Figs. 12** and **13** when the inlet is at the center of and at the rightmost position on the ceiling, respectively.

Fig. 14 shows an example of the flow distribution calculated by two dimensional and three dimensional schemes. Two dimensional computation was carried out in ψ-ω scheme with the equally spaced 16×16 mesh grid following the method described in the previous paper[1]. Three dimensional computation was done in u-p scheme with 10×10×10 mesh grid. The shape of the inlet and the outlet was slit. General features of the flow distribution agreed fairly well between two dimen-

sional and three dimensional computation. However, mixing factors were much higher in the three dimensional computation, as shown in **Fig. 15.** These results may indicate that mixing depends not only on the bulk pattern of the flow but also on small three dimensional perturbations.

From these results, it is clear that three dimensional computation is helpful and necessary for a quantitative estimation of ventilation efficiency. Furthermore, as the nature of the mixing factor is the same in both the two dimensional and three dimensional schemes, this factor can be eligible to be a suitable index of the ventilation efficiency.

Conclusion

1) There exists an optimum position for the inlet in relation to the outlet whereby the most effective ventilation can be obtained.
2) Similar to the case in two dimensions, the slope of the concentration decay is virtually constant and independent of the position in the room. So, the mixing factor derived from this slope would appear to be a good index of the ventilation efficiency.
3) Three dimensional computation seems to be necessary for a quantitative estimation of the mixing factor.

References

1) Y. Ishizu and K. Kaneki : Evaluation of Ventilation Systems through Numerical Computation and the Presentation of a New Ventilation Model, Trans. SHASE, No. 24(Feb., 1984), pp. 47～58
2) B. E. Lauder and D. B. Spalding : The Numerical Computation of Turbulent Flows, Comp. Method Appl. Mech. Engr., 3(1974), pp. 269～289
3) K. Yamaguchi : "Fundamental Study on Indoor Air Distribution", Doctoral thesis of Osaka University (in Japanese), (Jan., 1979)

(Received February 16, 1985)

三次元数値計算による換気システムの評価

石　津　嘉　昭*

等温，乱流，三次元のモデルで，給気口位置ならびに汚染物発生位置を変えた場合の気流分布と濃度分布を数値計算によって求め，換気効率が最も高くなる給排気口の最適位置関係を明らかにした．また，汚染物発生停止後の濃度減衰の傾きは室内のどの位置でもほぼ一定で，給排気口位置にのみ依存することから，この傾きによって換気効率が適切に表現できることを明らかにした．さらに，換気効率の定量的な評価にあたっては，三次元数値計算が必要であることも示した．

(昭和 60. 2. 16　原稿受付)

* 日本たばこ産業(株)中央研究所　正会員